# Naturally occurring Diels-Alder-type adducts from Morus nigra as potent inhibitors of Mycobacterium tuberculosis protein tyrosine phosphatase B

# Accepted Manuscript


Naturally occurring Diels-Alder-type adducts from *Morus nigra* as potent inhibitors of *Mycobacterium tuberculosis* protein tyrosine phosphatase B

Alessandra Mascarello, Angela Camila Orbem Menegatti, Andrea Calcaterra, Priscila Graziela Alves Martins, Louise Domeneghini Chiaradia-Delatorre, Ilaria D'Acquarica, Franco Ferrari, Valentina Pau, Adriana Sanna, Alessandro De Logu, Maurizio Botta, Bruno Botta, Hernán Terenzi, Mattia Mori

PII: S0223-5234(17)30990-X

DOI: 10.1016/j.ejmech.2017.11.087

Reference: EJMECH 9962

To appear in: *European Journal of Medicinal Chemistry*

Received Date: 13 June 2017

Revised Date: 14 November 2017

Accepted Date: 27 November 2017

Please cite this article as: A. Mascarello, A.C.O. Menegatti, A. Calcaterra, P.G.A. Martins, L.D. Chiaradia-Delatorre, I. D'Acquarica, F. Ferrari, V. Pau, A. Sanna, A. De Logu, M. Botta, B. Botta, Herná. Terenzi, M. Mori, Naturally occurring Diels-Alder-type adducts from *Morus nigra* as potent inhibitors of *Mycobacterium tuberculosis* protein tyrosine phosphatase B, *European Journal of Medicinal Chemistry* (2017), doi: 10.1016/j.ejmech.2017.11.087.

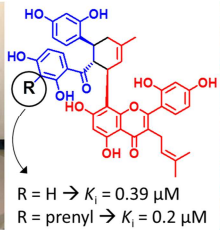


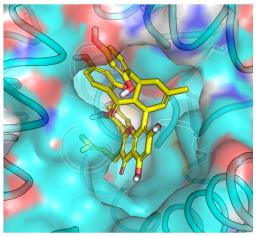

# Naturally occurring Diels-Alder-type adducts from *Morus nigra* as potent inhibitors of *Mycobacterium tuberculosis* protein tyrosine phosphatase B

Alessandra Mascarello,[#a,b] Angela Camila Orbem Menegatti,[#a] Andrea Calcaterra,[b] Priscila Graziela Alves Martins,[a] Louise Domeneghini Chiaradia-Delatorre,[a] Ilaria D'Acquarica,[b] Franco Ferrari,[b] Valentina Pau,[c] Adriana Sanna,[d] Alessandro De Logu,[c] Maurizio Botta,[e] Bruno Botta,[b] Hernán Terenzi,[a*] Mattia Mori[e,f*]

[a] *Centro de Biologia Molecular Estrutural, CEBIME−UFSC, Universidade Federal de Santa Catarina, Campus Trindade, 88040−900, Florianopolis − SC, Brasil.*

[b] *Dipartimento di Chimica e Tecnologie del Farmaco, Sapienza Università di Roma, P.le Aldo Moro 5, 00185, Roma (Italy)*

[c] *Dipartimento di Scienze della Vita e dell'Ambiente, Sezione di Scienze Farmaceutiche, Farmacologiche e Nutraceutiche, Università di Cagliari, Via Porcell 4, 09124, Cagliari (Italy)*

[d] *Department of Public Health, Clinical and Molecular Medicine, Università di Cagliari, Via Porcell 4, 09124 Cagliari (Italy)*

[e] *Dipartimento di Biotecnologie, Chimica e Farmacia, Università degli Studi di Siena, Via Aldo Moro 2, 53100, Siena (Italy)*

[f] *Center for Life Nano Science@Sapienza, Istituto Italiano di Tecnologia, Viale Regina Elena 291, 00161, Roma (Italy)*

[#] These authors contributed equally to this work

*__Corresponding Authors__: H.T. e-mail: *hernan.terenzi@ufsc.br*; M.M. e-mail: *mattia.mori@iit.it*

**ABSTRACT**

*Mycobacterium tuberculosis* (Mtb) protein tyrosine phosphatases A and B (PtpA and PtpB) have been recognized as potential molecular targets for the development of new therapeutic strategies against tuberculosis (TB). In this context, we have recently reported that the naturally occurring Diels-Alder-type adduct Kuwanol E is an inhibitor of PtpB ($K_i$ = 1.6 ± 0.1 µM). Here, we describe additional Diels-Alder-type adducts isolated from *Morus nigra* roots bark that inhibit PtpB at sub-micromolar concentrations. The two most potent compounds, namely Kuwanon G and Kuwanon H, showed $K_i$ values of 0.39 ± 0.27 and 0.20 ± 0.01 µM, respectively, and interacted with the active site of the enzyme as suggested by kinetics and mass spectrometry studies. Molecular docking coupled with intrinsic fluorescence analysis and isothermal titration calorimetry (ITC) further characterized the interaction of these promising PtpB inhibitors. Notably, in an Mtb survival assay inside macrophages, Kuwanon G showed inhibition of Mtb growth by 61.3%. All these results point to the common Diels-Alder-type adduct scaffold, and highlight its relevance for the development of PtpB inhibitors as candidate therapeutics for TB.

**Keywords**: PtpB inhibitors; tuberculosis; Diels-Alder-type adducts; natural products; kuwanones

## 1. INTRODUCTION

Tuberculosis (TB) is an infectious disease caused by the bacterium *Mycobacterium tuberculosis* (Mtb). According to the World Health Organization (WHO), there were almost 10.4 million new TB cases in 2015 (1 million of them were children) and 1.4 million TB deaths (140,000 were children), plus 0.4 additional deaths among people co-infected with HIV.[1] Accordingly, TB remains one of the top 10 causes of death worldwide in 2015. Patient noncompliance to the prescribed drugs is a critical factor that affects the success rate of conventional treatments against TB, leading to elevate the incidence of multidrug-resistant (MDR-TB), extensively drug-resistant (XDR-TB) and totally drug-resistant (TDR-TB) TB cases.[2] Thus, there is an urgent need for novel therapeutic targets for TB treatment, as well as new drugs and drug candidates that could act on them.

In this context, two protein tyrosine phosphatases (PTPs), namely PtpA and PtpB, which have been identified in Mtb's genome,[3] emerged a few years ago as profitable targets for the development of novel therapeutics against TB.[4-6] These enzymes are secreted by Mtb in infected human macrophages and are involved in the pathogen intracellular survival,[7] attenuating host innate immunity by interacting with host proteins such as TRIM27 and ubiquitin,[8, 9] as well as host signaling pathways including Jnk, p38, and NF-κB.[10] The mechanism of action of PtpA inside the host has been previously elucidated,[11, 12] whereas that of PtpB has only been suggested.[13, 14] Nevertheless, several reports substantiate that PtpA and PtpB inhibition by small molecules could impact Mtb survival in the host, thus paving the way for the development of innovative therapeutic strategies.[5, 12, 15-18]

The identification of Mtb PTPs inhibitors by screening campaigns or rational design has been addressed in the last decade,[17, 19-23] and natural products have played a key role in this field.[24] Indeed, natural products have long been recognized as an important source of therapeutically useful agents,[25-28] and can offer excellent opportunities for finding novel hits or leads against a broad

range of biological targets. In particular, our research group has assayed libraries of synthetic chalcone analogs to natural products, to find PtpA and PtpB inhibitors.[15, 29-31] Moreover, we have recently screened an *in house* library of natural compounds to find novel PtpB inhibitors,[31] by means of an integrated *in silico/in vitro* approach. This study identified Kuwanol E, a polyphenolic Diels-Alder-type adduct isolated from *Morus nigra* roots bark[32] (Figure 1) that is endowed with a noticeably inhibitory activity against PtpB ($K_i$ = 1.6 ± 0.1 μM).[31] Recently, the total synthesis of Kuwanol E has been reported.[33]

*Morus nigra* L. (family of *Moraceae*), also known as black mulberry, is one of the most important species of the genus *Morus*. The plants of this genus contain a variety of phenolic compounds including prenylated flavonoids, stilbenes, 2-arylbenzopyrans, coumarins, chromones, xanthones and Diels-Alder-type adducts.[32, 34-36] *M. nigra* and its constituents have been used in folk medicine as analgesic, anti-inflammatory, diuretic, antitussive, sedative, antimicrobial, cytotoxic, and antidiabetic agents.[36, 37] Some compounds isolated from the extract of the genus *Morus* have been explored in previous pharmacological studies, but only a few of them have been tested as modulators of purified proteins such as tyrosinase,[38-40] phosphodiesterase-4,[41] xanthine oxidase,[42] and α-glucosidase.[43, 44]

In addition, a few studies concerning compounds isolated from the *Morus* genus have highlighted their PTPs inhibition activity, specifically against the human phosphatase PTP1B. In particular, compounds isolated from *M. bombycs* showed $IC_{50}$ values ranging from 2.7 to 13.8 μM against the PTP1B, while the enzymatic kinetic assays suggested for these molecules a mixed-type mode of inhibition.[45] The inhibition of PTP1B by compounds isolated from *M. alba* was also investigated, highlighting an arylbenzofuran derivative as the most potent inhibitor, endowed with an $IC_{50}$ value of 7.9 μM.[43] More recently, Wang and co-workers evaluated the inhibitory activity of five compounds isolated from *M. notabilis* against PTP1B, showing $IC_{50}$ values ranging from 1.5 to 2.3 μM.[46]

In comparison with other species of the genus *Morus*, there are fewer studies involving the evaluation of biological and pharmacological properties of compounds isolated from *M. nigra*. Then, following our research interest in the discovery of natural compound inhibitors of Mtb PtpB, in this work, we present the results of an integrated study which combines enzyme inhibition and selectivity assays, kinetic and thermodynamic measurements, molecular modeling and evaluation of Mtb survival in human macrophages. Compounds isolated from *M. nigra* roots bark were considered, including flavonoids and Diels-Alder-type adducts. Our results provide further insights to establish this naturally occurring scaffold of potent and specific inhibitors of Mtb PtpB, and reinforce the druggability of PtpB in the development of anti-TB lead candidates.

## 2. RESULTS AND DISCUSSION

### 2.1. Preparation of *M. nigra* extracts, isolation and characterization of the natural compounds under investigation

A crude extract was obtained in acetone (8% yield) from the roots of *M. nigra* collected in the Riserva Naturale della Marcigliana, Rome (Italy). From this extract, the following compounds were isolated, with relative abundance reported in brackets: Kuwanon L (0.37%), Kuwanon G (5.8%), Kuwanon H (0.63%), Cudraflavanone A (0.66%), Morusin (2.1%), Oxyresveratrol (10%), Chalcomoracin (4.6%) and Norartocarpetin (0.15%) (Figure 1).

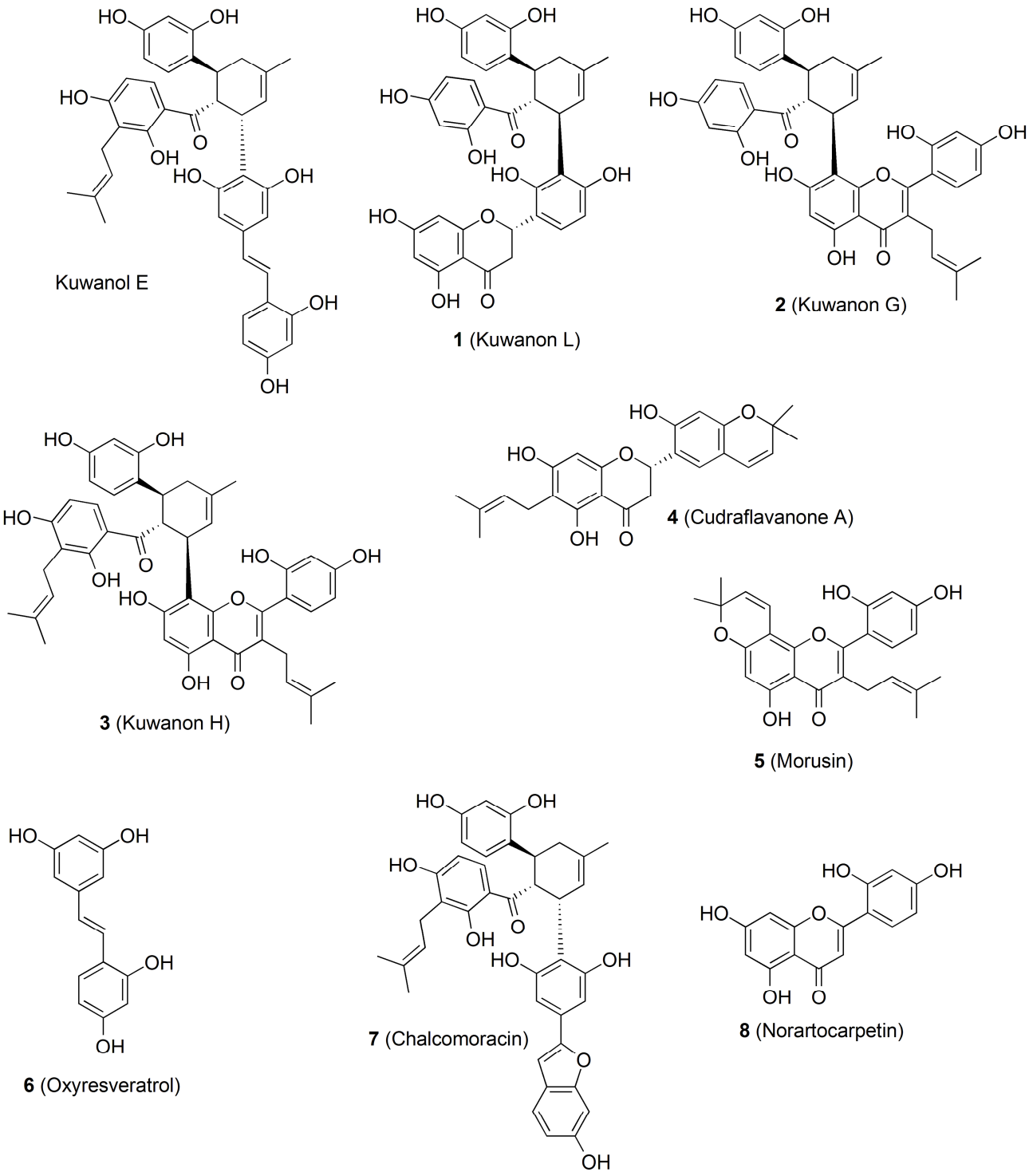


**Figure 1.** Chemical structure of small molecules isolated from *M. nigra.* Kuwanol E is the reference natural product inhibitor of PtpB, previously isolated from *M. nigra* roots bark;[31, 32] other natural compounds isolated from *M. nigra* and studied in this work are: Kuwanon L (**1**); Kuwanon G (**2**);

Kuwanon H (**3**); Cudraflavanone A (**4**); Morusin (**5**); Oxyresveratrol (**6**); Chalcomoracin (**7**); Norartocarpetin (**8**).

### 2.2. $IC_{50}$ determination of potential PtpB inhibitors

The inhibitory activity of compounds **1**–**8** (Figure 1) and the crude extract in acetone from *M. nigra* was evaluated towards recombinant PtpB using the method described previously.[31] All compounds showed significant inhibition of PtpB with $IC_{50}$ values ranging between 0.36 and 8.42 µM (Table 1). The best inhibitory effects were achieved by Kuwanon G (0.83 ± 0.35 µM, **2**, Figure 1) and Kuwanon H ($IC_{50}$ = 0.36 ± 0.05 µM, **3**, Figure 1), two polyphenolic Diels-Alder-type adducts that differ only for the presence of an additional prenyl group in Kuwanon H. Notably, this prenyl group is in the same position as found in the reference inhibitor Kuwanol E.[31] Among other Diels-Alder-type adducts, Chalcomoracin (**7**, Figure 1) also showed a satisfactory inhibition of PtpB with an $IC_{50}$ of 1.43 ± 0.22 µM, whereas Kuwanon L ($IC_{50}$ = 4.70 ± 1.12 µM, **1**, Figure 1), showed an activity 13-fold lower than that from Kuwanon H. It is worth mentioning that Chalcomoracin contains the same prenyl group as Kuwanol E and Kuwanon H, whereas Kuwanon L does not, thus suggesting that the presence of this prenyl group may be relevant for PtpB inhibition by this class of compounds.

Besides stereochemical configuration, the reference PtpB inhibitor Kuwanol E (Figure 1, $IC_{50}$ = 1.9 µM)[31] and Kuwanon G and H identified herein differ for the substituent to the cyclohexene ring: Kuwanol E bears an Oxyresveratrol moiety, whereas Kuwanon G and H share a flavone moiety. The different physicochemical features of these moieties provided ~5-fold and ~2-fold increase of inhibitory activity in Kuwanon H and G compared to Kuwanol E. The same trend was observed by testing the inhibitory effect of Oxyresveratrol (**6**, Figure 1), which showed the weakest inhibitory potency among the tested compounds ($IC_{50}$ = 8.42 ± 1.13 µM), whereas Norartocarpetin (**8**, Figure 1) which corresponds to the flavone moiety in Kuwanon L, G and H, showed a satisfactory inhibitory

activity against PtpB ($IC_{50}$ = 1.20 ± 0.25 µM), notably even better than the reference Kuwanol E. Finally, Morusin (**5**, Figure 1), and Cudraflavanone A (**4**, Figure 1) displayed moderate activity as PtpB inhibitors, with $IC_{50}$ values of 5.26 ± 0.22 µM and 5.07 ± 0.94 µM, respectively.

**Table 1.** *In vitro* inhibition ($IC_{50}$, µM) of isolated compounds **1**–**8** from *Morus nigra* against PtpB, PtpA, PTP1B, LYP, and PTP-PEST.

| Compound | PtpB | PtpA | SI* | PTP1B | SI** | LYP | SI*** | PTP-PEST | SI**** |
|---|---|---|---|---|---|---|---|---|---|
| **1** | 4.70 ± 1.12 | 13.96 ± 2.52 | 3.0 | 7.98 ± 0.66 | 1.7 | 12.12 ± 0.78 | 2.6 | 18.60 ± 0.84 | 3.9 |
| **2** | 0.83 ± 0.35 | 5.89 ± 0.81 | 7.1 | 4.56 ± 0.51 | 5.5 | 18.53 ± 1.44 | 22.3 | 12.41 ± 1.20 | 14.9 |
| **3** | 0.36 ± 0.05 | 1.49 ± 0.19 | 4.1 | 2.54 ± 0.29 | 7.0 | 11.75 ± 1.94 | 32.6 | 5.22 ± 1.00 | 14.5 |
| **4** | 5.07 ± 0.94 | 2.74 ± 0.77 | 0.5 | 4.31 ± 0.67 | 0.9 | 9.54 ± 1.16 | 1.9 | 18.61 ± 0.48 | 6.8 |
| **5** | 5.26 ± 0.22 | 4.65 ± 1.37 | 0.9 | 10.32 ± 1.74 | 2.0 | 14.97 ± 1.76 | 2.8 | >100 | >19 |
| **6** | 8.42 ± 1.13 | 67.23 ± 2.67 | 8.0 | 27.13 ± 0.52 | 3.2 | 31.45 ± 1.52 | 3.7 | >100 | >11.9 |
| **7** | 1.43 ± 0.22 | 2.43 ±0.32 | 1.7 | 1.94 ± 0.40 | 1.4 | 7.29 ± 0.82 | 5.1 | 8.52 ± 1.50 | 5.9 |
| **8** | 1.20 ± 0.25 | 11.97 ± 0.41 | 10.0 | 5.18 ± 0.81 | 4.3 | 30.29 ± 0.99 | 25.2 | 20.94 ± 0.53 | 17.5 |
| **#C. E. A.** | 1.48 ± 0.33 | 1.57 ± 0.27 | 1.1 | 1.24 ± 0.98 | 0.8 | 7.38 ± 0.41 | 5.0 | 7.41 ± 0.42 | 5 |

The results are shown as the average of the individual mean ± SD (standard deviation) for 3 experiments. SI = selectivity index. SI* = $IC_{50}^{PtpA}/IC_{50}^{PtpB}$; SI** = $IC_{50}^{PTP1B}/IC_{50}^{PtpB}$; SI*** = $IC_{50}^{LYP}/IC_{50}^{PtpB}$; SI ****= $IC_{50}^{PEST}/IC_{50}^{PtpB}$.

# C.E.A. = crude extract in acetone..

In order to define the PTPs inhibition profile of natural products **1**–**8** and the crude extract, their effects on the catalytic activity of Mtb PtpA and human PTP1B, PTP-PEST (also referred as PTPN12; PTP-proline-, glutamic acid-, serine- and threonine-rich (PEST)), and LYP (Lymphoid-specific tyrosine phosphatase) were also investigated. The selectivity index (SI) was then calculated as the ratio between

the $IC_{50}$ measured against other PTPs and the $IC_{50}$ measured against the target Mtb PtpB. As shown in Table 1, Kuwanon G and H showed a moderate specificity for PtpB over PtpA and PTP1B with SI values in the range 4.1 – 7.1, whereas a good selectivity of these compounds for PtpB over LYP and PTP-PEST was observed, with SI values in the range 14.5 – 32.6. Although we are aware that the tested panel of phosphatases is not exhaustive, these results suggest that Kuwanon G and H are potent inhibitors of PtpB, and that they are endowed with a certain specificity for PtpB among a panel of relevant PTPs.

**2.3. Enzyme kinetic analysis**

The two most potent PtpB inhibitors Kuwanon G and H were selected for further enzyme kinetic analysis. The Michaelis-Menten plots (Figure 2) indicate that these two compounds caused increases in apparent $K_m$ values with the rise of inhibitor concentrations. On the other hand, the $V_{max}$ value remains constant to Kuwanon H, indicating a competitive mechanism of inhibition, while to Kuwanon G, in the inhibitor presence, we observed a small reduction in the $V_{max}$ values. However, the velocities did not decrease curvilinearly as expected for a non-competitive inhibition with $\alpha > 1$, the $V_{max}$ values were similar for the three concentrations of inhibitor. As the velocity in the presence of a competitive inhibitor may be considered equal to $V_{max}$ values when the substrate concentration is $\geq 100K_{m\ app,}$ the above-mentioned kinetics were fitted to a Michaelis-Menten with a competitive inhibition model.[47] The $K_i$ values obtained for Kuwanon G and Kuwanon H were 0.39 ± 0.27 and 0.20 ± 0.01 μM, respectively. In order to support the mechanism of inhibition, we also studied the relationship between $IC_{50}$ and the substrate concentration of Kuwanon H. The $IC_{50}$ of Kuwanon H was dependent on the *p*NPP concentration; excess of substrate did effectively compete with inhibitor, which ratifies a competitive inhibition mechanism (see Supporting Information Figure S1A). Furthermore, to determine whether the compounds cause the enzyme inactivation or reversible inhibition, acting as a fully

reversible, slowly reversible, or irreversible inhibitors, PtpB inhibition by Kuwanon G and H was measured using a preincubation/dilution assay.[47] After the 100-fold dilution of the enzyme-inhibitor complex (preincubation following an equilibration time of 30 min at 37 °C) approximately 40% of PtpB activity was recovered compared to the free protein, for both compounds (see Supporting Information Figure S1B). Such result might suggest the behavior of slowly dissociating inhibitors. In addition, PtpB inhibition by these compounds was independent on the incubation time, at a concentration of 0.2 μM (see Supporting Information Figure S1C), which could indicate a rapid binding event.

Next, we pursued to define the mechanism of inhibition of the human ortholog PTP1B by Kuwanon G, which showed a SI value of 5.5 compared to Mtb PtpB (namely, the lowest value found among the human PTPs evaluated in this work, see Table 1). Using a steady-state inhibition kinetics, we found that Kuwanon G is a non-competitive inhibitor of PTP1B, producing a reduction in $V_{max}$ with little or no effect on $K_m$ (Figure 2). This data suggests that, compared to PtpB, Kuwanon G binds in an allosteric site of human PTP1B. The mentioned kinetics were fitted to a Michaelis-Menten with a non-competitive inhibition model, providing a $K_i$ value of 10.2 ± 2.0 μM for PTP1B inhibition that is 26-fold higher than that observed against PtpB (0.39 ± 0.27 μM).

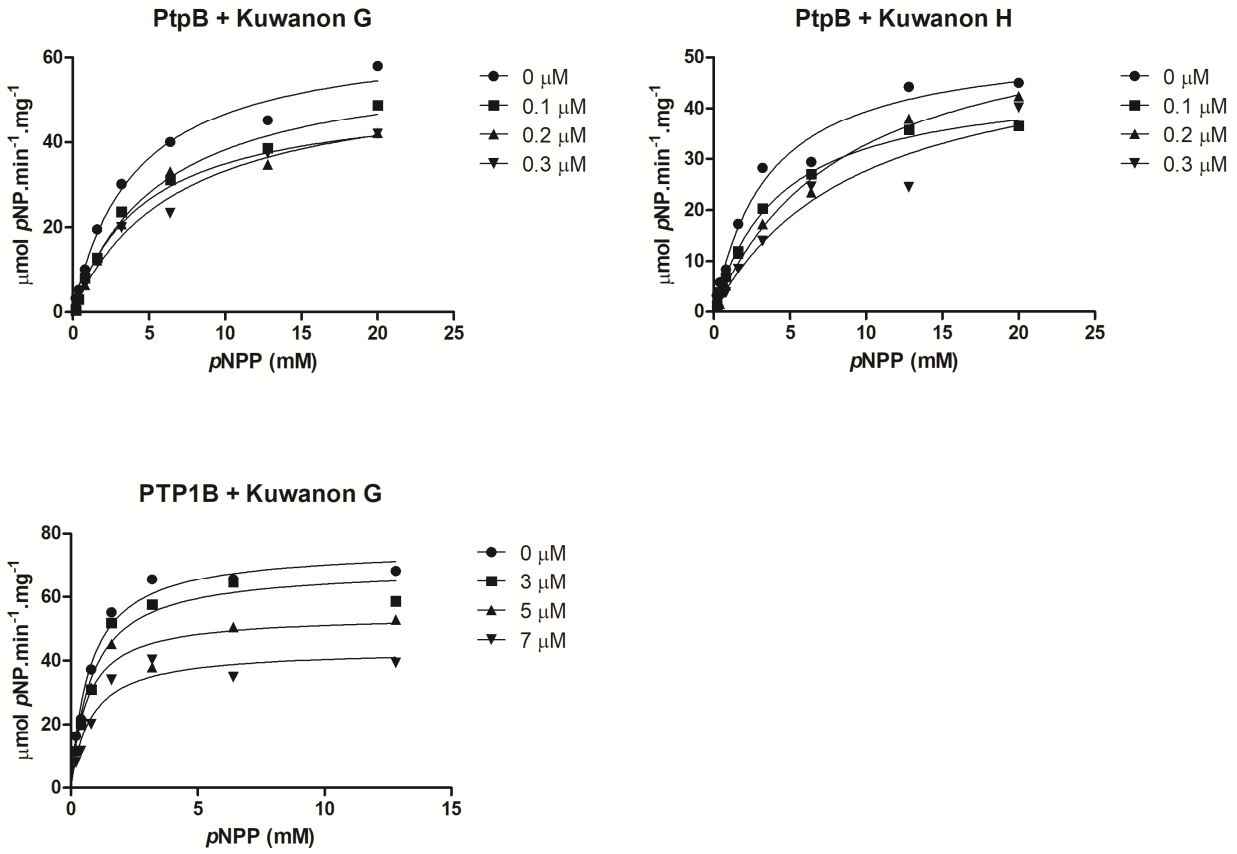


**Figure 2**. Inhibition kinetics of Mtb PtpB by Kuwanon G and H, and human PTP1B by Kuwanon G. Michaelis-Menten plots of kinetic analysis of Kuwanon G and Kuwanon H are showed in the respective panels. The $K_i$ values were determined from 3 independent measurements.

### 2.4. PtpB intrinsic fluorescence: effects triggered by Kuwanon G and Kuwanon H

According to its primary sequence and three-dimensional structure, PtpB possesses a tryptophan residue (Trp10), and 6 tyrosine residues (Tyr).[48] The Trp10 and four out of the six tyrosine residues are found in the catalytic domain and, among them, Trp10 is the most dominant fluorophore. The fluorescence spectrum of PtpB presents an emission maximum ($\lambda_{max}$) at 330 nm, when excited at 280 nm or 295 nm, as expected for a buried tryptophan.[49] The tyrosine residue 125 (Tyr125) in the α-helix 4 was previously shown to be important for (oxalylamino-methylene)-thiophene sulfonamide

(OMTS) binding to PtpB;[20] furthermore, we previously reported that Kuwanol E establishes H-bond interactions with such residue.[31] Accordingly, the binding of Kuwanon G and H to PtpB was further investigated by monitoring the intrinsic fluorescence of the protein. The fluorescence spectra were recorded in different concentrations of the compounds, following excitation at 280 nm (monitoring Trp and Tyr excitation) or 295 nm (monitoring only the Trp excitation) as shown in Figure 3, and in Supporting Information Figures S2 and S3**.** The addition of the compounds resulted in fluorescence quenching without a shift in the $\lambda_{max,}$ indicating that the global structure of PtpB and the local environment of the tryptophan residue, is not altered by the interaction with the compounds in both conditions (namely, excitation at 280 nm or 295 nm).

To investigate the mechanism of fluorescence quenching, we performed UV-vis measurements of PtpB in the absence or presence of the compounds (see Supporting Information Figure S4). We observed that the addition of compounds caused the increase in the absorption at 280 nm and between 310 to 350 nm, thus both compounds changed the absorption spectrum of PtpB, suggesting that the fluorescence quenching is static, owing to the formation of the protein-inhibitor complex.[49] The equilibrium binding of Kuwanon G and H to PtpB was followed by the change in protein fluorescence signal upon inhibitor binding. The fluorescence data collected was analyzed with the modified Stern−Volmer (SV) equation 1 (see Experimental Section), using the *log* of fluorescence intensity at spectral maxima *vs log* of inhibitor concentration. The plots are shown in Figure 3C-D and in Supporting Information Figure S2E-F. Analysis of quenching data for both Kuwanon G and H resulted in almost identical equilibrium dissociation constants ($K_d$) (excitation at 280 nm), in agreement with the kinetic inhibition constants previously obtained, with $K_i$ values of 0.39 ± 0.27 and 0.20 ± 0.01 μM, respectively. In addition, our data suggest that both inhibitors have only a single binding site in PtpB (equation 1 in Experimental Section). As shown in Table 2 and S1, Kuwanon G and H binding parameters obtained following Trp and Tyr (at 280 nm) or only the Trp excitation (295 nm) showed similar values.

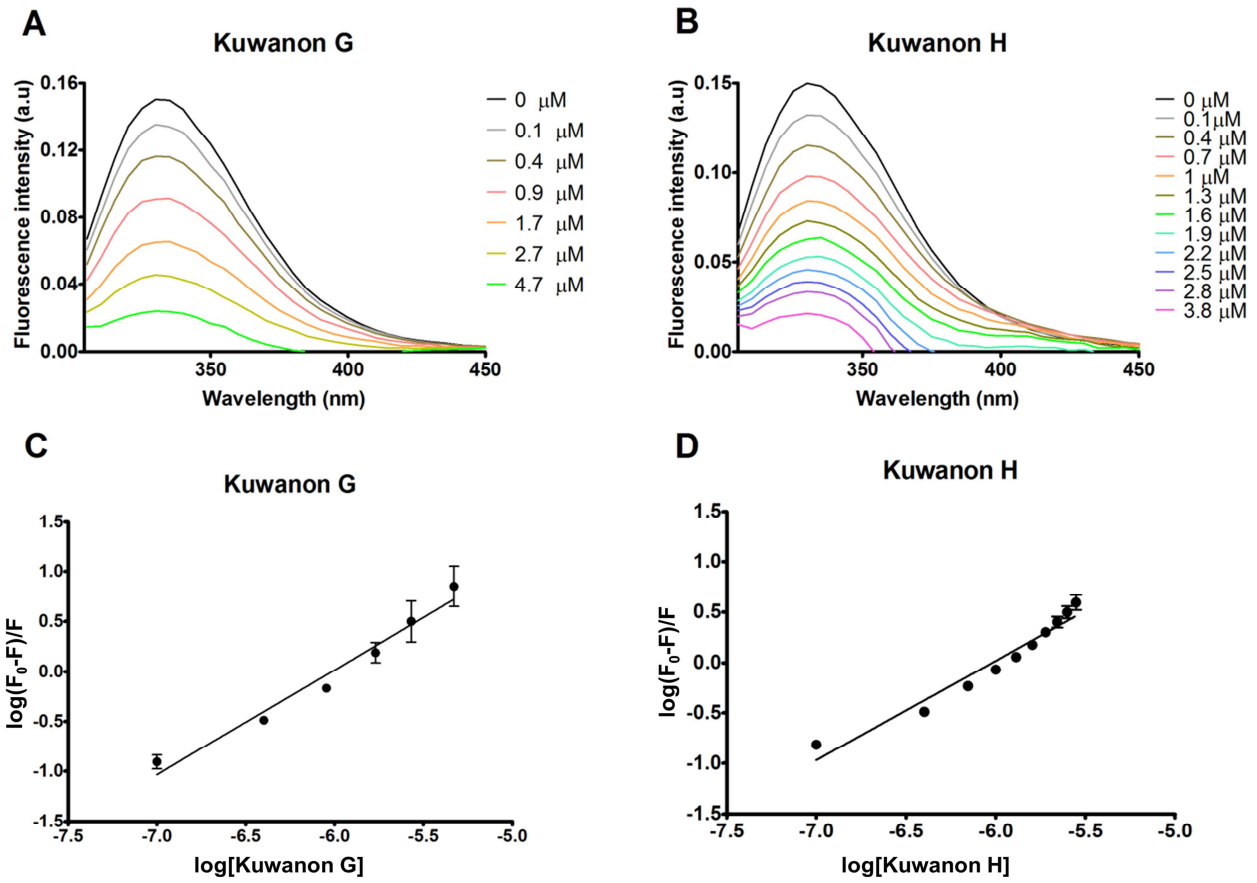


**Figure 3**. Representative fluorescence quenching spectra of PtpB at different concentrations of inhibitors. Steady-state fluorescence emission spectra of PtpB in the presence of increasing concentrations of Kuwanon G (A) and H (B), excitation at 295 nm. Plots of *log*($F_0$−F)/F *versus log* of Kuwanol G and H concentration (C and D, respectively). The data represent the average ± SE of two independent experiments.

**Table 2.** Comparison of binding parameters measured by intrinsic fluorescence.

| **Compound** | **N, sites** | $K_a$, $M^{-1}$ | [a] $K_d$, µM | [b] ΔG, kcal $mol^{-1}$ |
|---|---|---|---|---|
| Kuwanon G | 1.0 ± 0.2 | 1.0 ± 0.2 x $10^6$ | 1.0 ± 0.2 | -8.2 ± 0.1 |

| | | | | |
|---|---|---|---|---|
| Kuwanon H | 1.0 ± 0.1 | 1.0 ± 0.07 x $10^6$ | 1.0 ± 0.07 | -8.2 ± 0.05 |

Parameters obtained using equation 1 (see Experimental Section). Excitation at 295 nm. [a]$K_a = 1/K_d$, [b]$\Delta G = -RT\ln K_a$. The data represent the average of two independent experiments

**2.5. Thermodynamic analysis of Kuwanon G binding to PtpB**

The binding of Kuwanon G to PtpB was also measured using isothermal titration calorimetry (ITC) in an attempt to divide the binding energy into enthalpic and entropic components, and to obtain the dissociation constants and the stoichiometry of the interaction. ITC was not performed on Kuwanon H, since the compound is not soluble in the necessary experimental conditions.

Figure 4 shows the interaction between Kuwanon G and PtpB. The ITC data could be fitted according to a single-site binding model (a 1:1 equilibrium), also supported by fluorescence quenching experiments (Figure 3), and the thermodynamic parameters of binding are summarized in Table 3. The analysis showed favorable binding parameters for Kuwanon G ($\Delta G$ = -7.5 ± 0.1 kcal $mol^{-1}$), in agreement with the previous observations (Table 2), and the binding isotherm leads to $K_d$ = 2.9 ± 0.4 μM. The dissociation constant determined by ITC was ~2-fold higher than that obtained from the previous fluorescence quenching analysis, although within the same order of magnitude. The binding of Kuwanon G was found to be exothermic with favorable enthalpic and unfavorable entropic contributions (Table 3). In fact, the free energy of binding is clearly dominated by an enthalpic component (Figure 4), since at 25 °C the entropic contribution ($T\Delta S$) to the overall free energy is equal to −6.2 ± 0.8 kcal $mol^{-1}$ whereas the enthalpic contribution ($\Delta H$) is equal to −13.7 ± 0.7 kcal $mol^{-1}$, suggesting that the binding predominantly involves the formation of H-bonds in addition to small conformational changes. The thermodynamic profile for the binding of Mtb β-ketoacyl CoA reductase FabG4 to a triazole polyphenol hybrid compound (in this case a competitive inhibitor) revealed that the interaction is governed by strong H-bonding (with Asp, Arg and Asn residues) and conformational

changes, supported by the negative ΔH and ΔS parameters and also corroborated by docking studies.[50] In addition, the binding study of two structurally similar ligands to human histone deacetylase 8 (HDAC8) showed that the inhibitor with an enthalpic gain (higher negative ΔH), as a result of a specific hydrogen bond in the active site of HDAC8, as well as an entropic penalty caused likely by a reduction in the conformational flexibility, tends to be more target-specific.[51] Overall, these results coupled with kinetics and fluorescence quenching studies indicates that Kuwanon G binds directly to the protein, most likely within the catalytic active site. Moreover, recent studies have demonstrated that inhibitors where the enthalpic contribution dominates the binding events may be the best candidates to lead optimization since a few strong hydrogen bonds can improve selectivity and specificity for the target molecules.[51, 52]

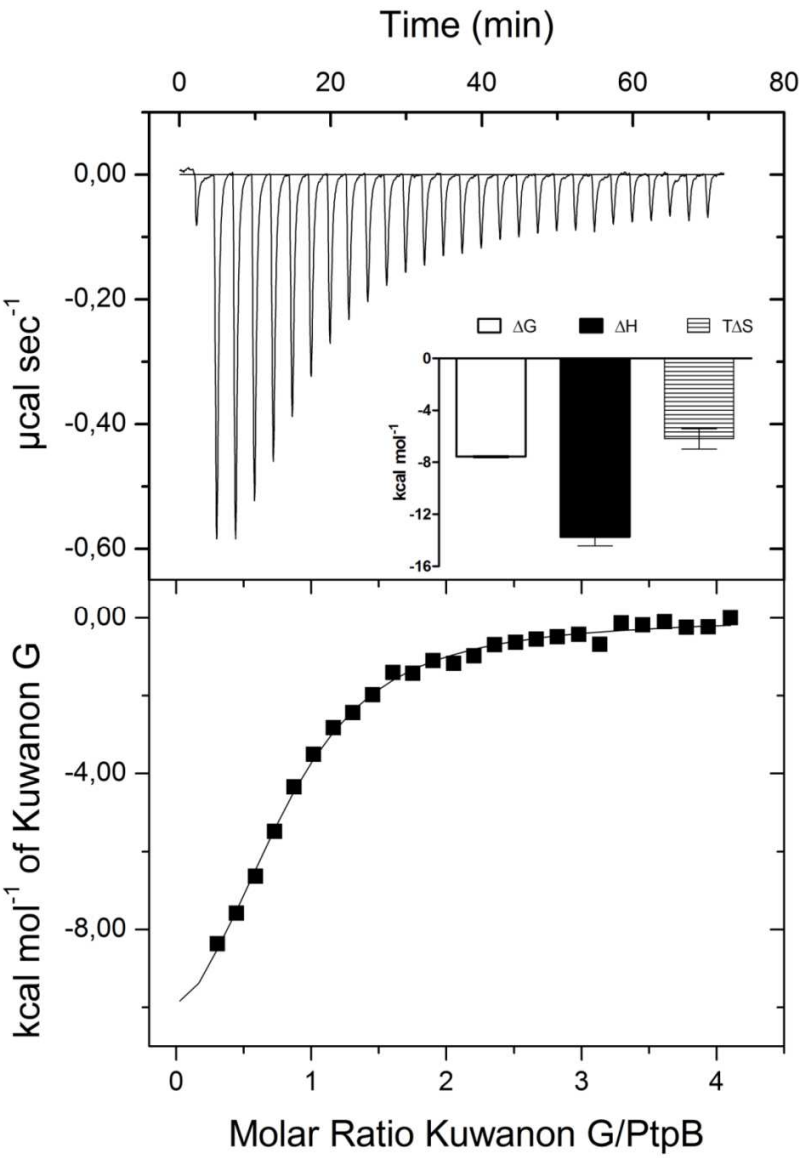


**Figure 4.** Isothermal titration calorimetry (ITC) of Kuwanon G binding to PtpB. Inset, the thermodynamic profile of the binding. The titration was performed at 25 °C with 10 µM PtpB in the cell and 200 µM Kuwanon G in the syringe. In the representative figure (two independent experiments) the upper panel displays the raw ITC data, and the normalized data, corrected for the control dilution heat, is shown in the lower panel.

**Table 3.** Thermodynamic parameters for the binding of Kuwanon G to PtpB.

| N, sites | $K_a$, $M^{-1}$ | ΔH, kcal $mol^{-1}$ | ΔS, cal $mol^{-1}$ $K^{-1}$ | [a]ΔG, kcal $mol^{-1}$ |
|---|---|---|---|---|
| 0.9 ± 0.1 | 3.5 ± 0.5 x $10^5$ | -13.7 ± 0.7 | -20.8 ± 2.6 | -7.5 ± 0.1 |

10 μM of PtpB titrated with 200 μM Kuwanon G at 25 °C. [a]$\Delta G = -RT\ln K_a$. The data presented are the average, with standard deviations, from two independent experiments

### 2.6. PtpB proteolysis protection by Kuwanon G and H

In order to investigate the possible binding site of Kuwanon G and H, we analyzed PtpB peptide mass fingerprint (PMF) in the presence or in the absence of the inhibitor. In the case of free PtpB, approximately 92% of its sequence was covered by PMF (Figure 5A). As shown in Figure 5B-C, pre-incubation of PtpB with Kuwanon G or Kuwanon H led to several changes in the cleavage profile. The main differences compared to the free PtpB are intensity decrease or the disappearance of the signals of fragments related to the substrate binding region, and the increase in the intensity of fragments located far from the active site. In the presence of 100 μM Kuwanon G, we observed about 90% sequence coverage of PtpB; furthermore, the intensity of the two fragments at *m/z* 1953 and *m/z* 2224 that correspond to the amino acids sequence of the active site (residues 146-166) was markedly reduced (Figure 5B, and Supporting Information Figures S5 and S6). On the other hand, novel signals appeared in the PMF profile of PtpB in the presence of Kuwanon G, namely four new fragments at *m/z* 1305, *m/z* 1761, *m/z* 2430, and *m/z* 2785, while seven fragments increased their intensity (Supporting Information Figures S7-S15). These segments include the his-tag sequence, the α-helices 1, 8, 9 and 10, β-sheet 2 and 4, and a small portion of α-helices 2, 4, 5, 7 and 11, which are oriented outwards, surrounding the active site (Supporting Information Figure S16A). Interestingly, the fragment at *m/z* 2430 (that appears only in the presence of the inhibitor) covers the amino acids residues 141-164, which includes part of catalytic site, but compared to fragments *m/z* 1953 and *m/z* 2224 this sequence covers a larger region of

α 5 helix (Supporting Information Figure S17). This result suggests that even during the course of the proteolysis experiment, if trypsin reaches the active site region it does not seem to have free access to all the amino acid residues of this region, since the intensity of the fragments *m/z* 1953 and *m/z* 2224 were reduced, indicating that the compounds interact with other surface determinants of the active site of the enzyme.

In the presence of 100 μM Kuwanon H, we also observed about 93% sequence coverage of PtpB and the strong intensity reduction of the fragment *m/z* 1953, besides the disappearance of the fragment at *m/z* 2224 (Figure 5C, and Supporting Information Figures S5, S6). As observed for Kuwanon G, novel signals appeared in the PMF profile of PtpB in the presence of Kuwanon H, namely five new fragments at *m/z* 1243, *m/z* 1305, *m/z* 1761, *m/z* 2785, and *m/z* 2809, while ten fragments increased their intensity (Supporting Information Figures S7, S8, S10-15, S18, S19). As shown above, these segments include the his-tag sequence, the α-helices 1, 2, 8, 9, 10, β-sheet 2 and a small portion of α-helices 4, 7 and 11 (Supporting Information Figure S16B).

These data indicate that both Kuwanon G and H are able to protect the active site from proteolytic cleavage of trypsin in a very similar manner, thus allowing trypsin to cleave more efficiently other PtpB segments as observed in PMFs. Taking into account the increased intensity observed for the fragment related to the his-tag and other fragments around the active site, as well as the presence of protein fragments not previously seen in the absence of the compound, we assume that inhibitor binding might alter trypsin accessibility to PtpB. These results further indicate that Kuwanon G and H may bind within the catalytic active site of PtpB.

Kinetics results described in 2.3 suggest that Kuwanon G does not interact with the active site of PTP1B, which is consistent with its non-competitive mechanism of inhibition. To further corroborate this data, PTP1B PMF profile was analyzed in the presence or in the absence of Kuwanon G (Supporting Information Figure S20). Notably, we did not observe significant differences in the

intensity of the fragments with *m/z* 2175 or *m/z* 2430 (Supporting Information Figure S21) that correspond to the amino acids sequence of the active site and P-loop (residues 198-221). Different from what observed against the mycobacterial PtpB, inhibition of human PTP1B by Kuwanon G may not require direct binding of the compound to the catalytic site of the enzyme. As shown in Figure S22-26, the main differences found in the PTP1B digestion profile in the presence of Kuwanon G compared to the free enzyme were: i) the intensity decrease of the signals of fragments related to the C-terminal tail, the α-helices 4 (fragments at *m/z* 1730 and *m/z* 1886) and 6 (fragments at *m/z* 1197, *m/z* 1245), and ii) the increase in the intensity of fragments located at the N-terminal tail, β-sheet 1 (fragments at m/z 1059 and m/z 2758) near the second phosphate binding site, the YRD signature motif.[53] Wiesmann and co-workers identified an allosteric pocket on PTP1B that is located near the C-terminal tail, flanked by helices α3, α6 and α7.[54] X-ray crystallography studies revealed that the potential mechanism for allosteric inhibition is to prevent the formation of catalytic competent PTP1B active site by restraining the WPD-loop (Trp179, Pro180 and Asp181) in the open conformation. In addition, Krishnan and co-workers have characterized another non-competitive inhibitor, MSI-1436, that binds at the C-terminus of PTP1B, with some similarities to the allosteric binding site.[54-57] Since the intensity of the fragments *m/z* 1197, *m/z* 1245 (residues 258-279 in the helices α6) was reduced, indicating a potential protection of this region by the inhibitor, we hypothesized that Kuwanon G could bind near the allosteric binding site with different affinity and mechanism when compared to PtpB. However, further analysis are needed to understand the binding of the Kuwanon G to PTP1B, in order to exploit structural features for gaining selectivity for PtpB or PTP1B in the optimization of Kuwanon G.

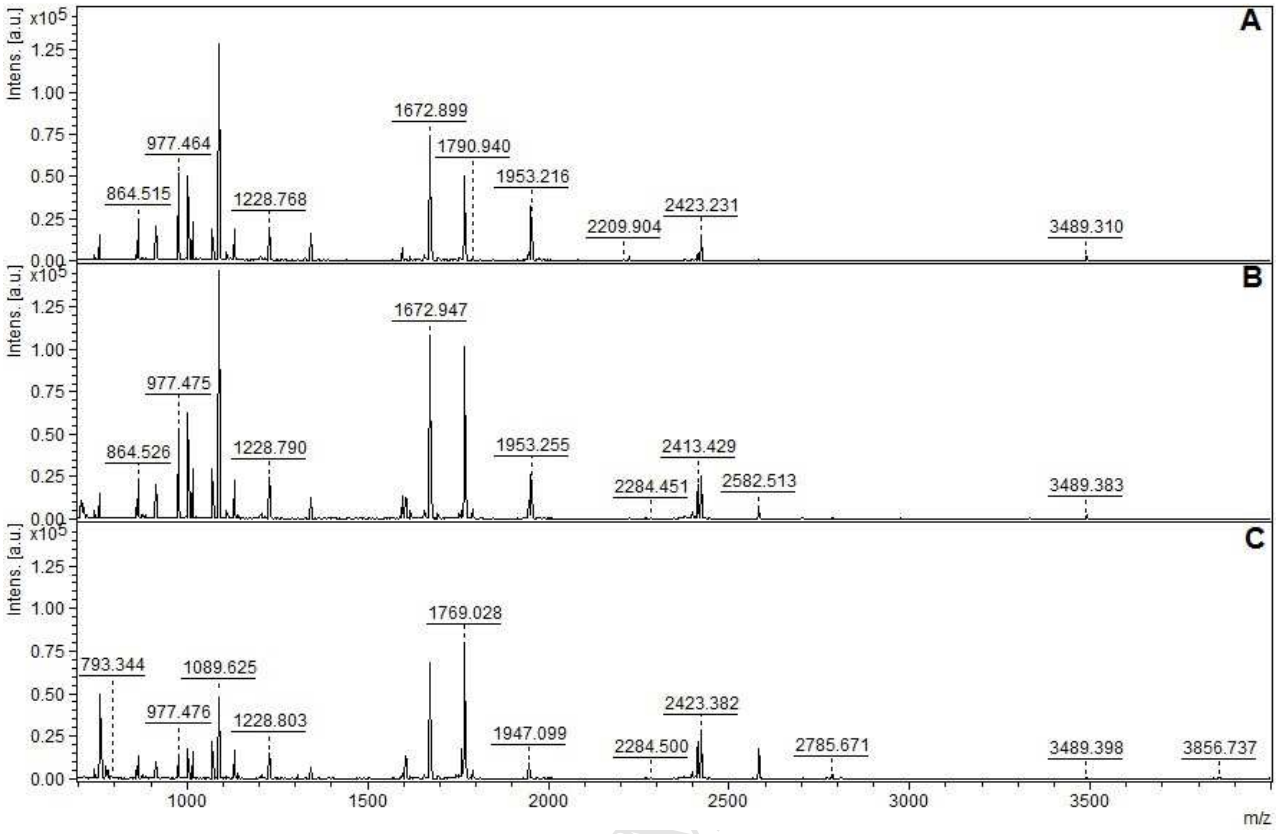


**Figure 5.** Peptide mass fingerprint profile of PtpB recorded in the absence (A) and in the presence of Kuwanon G (B) and Kuwanon H (C). The protein (5 μM) was digested with trypsin (1:50 molar ratio) for 3 hours at 37 °C in the absence or presence of inhibitor (100 μM).

### 2.7. Molecular modeling

To further corroborate the results obtained *in vitro,* and to attempt a structure-based rationalization of experimental evidences, the binding mode of newly identified PtpB inhibitors was predicted by molecular modeling. To this end, the protocol already described previously was used herein.[31] All the molecules in Figure 1 were able to fit the catalytic active site of PtpB. The binding mode of Kuwanon G and H is shown in Figure 6 and described in deeper details below while the binding mode of weaker PtpB inhibitors is shown in Supporting Information Figure S27.

As expected based on the chemical structure, Kuwanon G and H bind in a similar manner to PtpB active site, and establish H-bonds with the catalytic residue Cys160, as well as with the side chain of Tyr125, Asp165, Arg166, and a crystallographic water molecule (residues numbering is that of the crystallographic structure coded by PDB ID: 2OZ5).[14] Besides polar contacts, the two Diels-Alder-type adducts establish hydrophobic interactions with Phe98, Leu101, Tyr125, Met126, Phe161, Leu199, Ile203, Met206, Leu227, Val231, and Leu232. As highlighted above, the only difference between Kuwanon G and H is the presence of an additional prenyl group in Kuwanon H. This group was predicted to interact with Phe166 by molecular docking, thus becoming potentially responsible for the slightly higher affinity and lower $IC_{50}$ value observed experimentally for Kuwanon H compared to Kuwanon G. This prenyl group may also be responsible for the lower solubility of the molecule in aqueous media, as observed in ITC measurements. Finally, the predicted binding mode is in agreement with the evidence of a single binding site for Kuwanon G and H within PtpB catalytic domain, as emerged from the analysis of PtpB intrinsic fluorescence discussed above.

Matching theoretical affinities with experimental $-\log IC_{50}$ values provided a satisfactory correlation that further reinforces the reliability of the computational protocol as well as of the predicted binding modes ($R^2 = 0.48$ for the whole test set, and $R^2 = 0.85$ after leaving out the underestimated scoring value of the Norartocarpetin, see also Supporting Information Figure S28 and Table S2).

To provide a structural support to the inhibitory activity of Kuwanon G towards the human ortholog PTP1B, and to drive further optimization of this lead candidate up to a more selective PtpB inhibitor, the predicted binding mode of Kuwanon G to PTP1B was also predicted by molecular docking. In agreement with PMF results, which ruled out the binding of Kuwanon G to the active site, molecular docking with GOLD proved unable to find a suitable binding pose of Kuwanon G within the narrow catalytic cavity of PTP1B in contact with key catalytic residues (data not shown). In contrast, and in agreement with PMF data, Kuwanon G was successfully docked in the allosteric binding site that is

located near the C-terminal tail of PTP1B, flanked by helices α3, α6 and α7.[54] Notably, the predicted binding mode of Kuwanon G shows moderately good overlapping with the crystallographic binding mode of a benzofuran allosteric inhibitor (Supporting Information Figure S29). Although additional efforts should be spent to characterize the binding of Kuwanon G to PTP1B, the predicted binding mode is in agreement with experimental data and may represent a valuable starting point in further lead optimization efforts.

In summary, molecular modeling results are in good agreement with *in vitro* data and further elucidate the molecular details of the inhibitory activity exerted by Kuwanon G and H against Mtb PtpB, and by Kuwanon G against the human ortholog PTP1B.

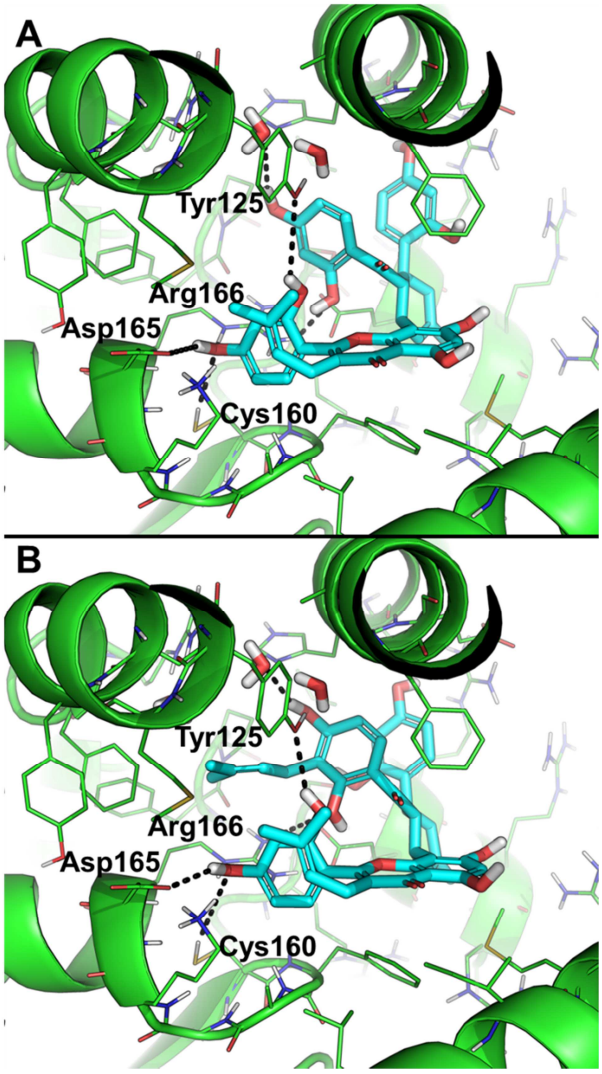

**Figure 6.** Predicted binding mode of the two most potent PtpB inhibitors. Kuwanon G (A) and Kuwanon H (B) are showed as cyan sticks. The crystallographic structure of PtpB is shown as green lines and cartoon. Residues involved in H-bonding to the inhibitors are labeled, and H-bonds are indicated as dashed lines.

### 2.8. MIC, cytotoxicity and macrophage assay

To assess the translational potentiality of Kuwanon G and H, their efficacy in inhibiting the growth and replication of Mtb was evaluated *in vitro*. First, the MICs against Mtb H37Ra were determined by the resazurin microtiter assay, providing a value of 32 µg/mL for both Kuwanon G and Kuwanon H. Notably, these molecules showed cytotoxicity in THP-1 cells at concentrations that are highly comparable to the observed MICs ($CC_{50}$ values of 33.77 and 20.23 µg/mL for Kuwanon G and Kuwanon H, respectively, as determined by the MTT reduction assay). Therefore, in evaluating TB survival inside macrophages, we used the non-toxic concentration of 10 µg/mL (corresponding to 14.4 and 13.2 µM of Kuwanon G and H, respectively). However, at this concentration, Kuwanon H was inactive, whereas Kuwanon G still showed an inhibition of Mtb growth by 61.3% with respect to the untreated control. This data, in particular, is worthy of note since such inhibition occurred at non-toxic concentrations that are also much lower than the MIC values. Overall, the results of this biological investigation highlight the relevance of the Diels-Alder-type adduct Kuwanon G isolated from *Morus nigra* as candidate anti-TB lead compound.

## 3. CONCLUSIONS

Examination of the roots of *M. nigra* and subsequent analysis of the PtpB inhibitory activities of the purified components yielded preliminary structure-activity relationship data, which might be useful for future studies in this area. Some of tested compounds were potent inhibitors of this protein, indicating

that constituents from *M. nigra* roots could be promising natural agents to counteract phosphatase activity and inhibit the growth of Mtb. In particular, the naturally occurring Diels-Alder-type adducts Kuwanon G and Kuwanon H are potent inhibitors of Mtb PtpB, and their mechanism of action was herein characterized by an integrated approach that combines biochemical tool with molecular modeling and *in vitro* assays. Kuwanon G was also found to inhibit the human ortholog PTP1B, albeit to a lesser extent and with a different mechanism of action (i.e. non-competitive inhibition) compared to Mtb PtpB, which suggests a possible strategy to further optimize Kuwanon G up to a highly selective PtpB inhibitor. Notably, Kuwanon G proved to inhibit the growth of Mtb in infected macrophages at low micromolar non-toxic concentrations, thus becoming a successful lead candidate for future development as well as for further understanding the role of PtpB in Mtb infection.

## 4. EXPERIMENTAL SECTION

### 4.1. Preparation of the extracts, isolation and characterization of the compounds

The roots of *M. nigra* (10 kg) were collected in the Riserva Naturale della Marcigliana, Rome (Italy), in the summer, and air-dried for 15 days. Once the bark (1.2 kg) was obtained from the roots, it was exhaustively extracted with acetone (6L, r.t.) for 15 days and the residue was subjected to column chromatography (CC) on silica gel 60 (70-270 mesh, 40 x 40 mm) and eluted under gradient conditions with methanol:$CHCl_3$. The fractions obtained were further purified by CC over silica gel using *n*-hexane in ethyl acetate also under gradient conditions. Finally, the crude compounds were further purified by reversed-phase medium-pressure liquid chromatography (RP-MPLC) in water:methanol 20:80, according to Ferrari and co-workers.[32] The NMR and mass spectrometry data for the isolated compounds were coincident and in agreement with those already reported for Kuwanon L (**1**);[58-60]

Kuwanon G (**2**);[59, 60] Kuwanon H (**3**);[60, 61] Cudraflavanone A (**4**);[62] Morusin (**5**);[60, 61] Oxyresveratrol (**6**);[60, 63] Chalcomoracin (**7**);[64, 65] Norartocarpetin (**8**).[66, 67]

The purity of compounds (≥ 95%) was checked by analytical HPLC. Column: Phenomenex Luna C18 (250 × 4.6 mm i.d., Torrance, CA, USA). Mobile phases A: $H_2O$/MeCN = 90:10 (v/v); B: MeCN. Gradient elution: at 30% B for 5 min; to 100% B in 15 min (linear); at 100% B for 5 min; to 30% B in 5 min. Flow rate: 1.0 mL/min. PDA detection at 280 nm.

**4.2. PTPs expression and purification**

PtpB and PtpA from *Mycobacterium tuberculosis* and human PTP1B expression and purification were performed as previously described.[30] LYP and PTP-PEST were expressed and purified by the same method described for PtpA and PtpB, with the following modification, expression was induced with 0.5 mM isopropyl β-D-thiogalactopyranoside (IPTG) and the cells were incubated overnight at 25 °C.

**4.3. Measurement of PTPs inhibition ($IC_{50}$)**

The phosphatase assays were carried out as previously described,[31] in a total reaction volume of 200 µL containing 20 mM imidazole pH 7.0, different concentrations of the inhibitor (in a solution containing 4% dimethyl sulfoxide - DMSO), 30 nM PtpB (2 µL in 20 mM Tris–HCl pH 8.0, 50 mM NaCl, 5 mM EDTA, 20% glycerol, and 5 mM DTT) and 20 mM *p*-nitrophenyl phosphate (*p*NPP). The compound was premixed with PtpB for 10 min at 37 °C, and the reaction was started by addition of *p*NPP. The absorbance was measured with a UV-vis spectrophotometer in 96-well plates (TECAN Magellan Infinite M200) for 10 min at 37 °C (at 410 nm with readings every 1 min). Positive controls were performed in the absence of compounds and 4% DMSO. The experimental data were analyzed with GraphPad Prism 5.0 and the $IC_{50}$ values determined by linear regression. All assays were performed in triplicate. The PTPs inhibition profile of tested molecules was carried out using 2 µL of recombinant LYP (169 nM), PTP-PEST (205 nM), PTP1B (38 nM) and PtpA (92 nM), under the same conditions used for PtpB.[31]

### 4.4. Enzyme kinetics

The mechanism of inhibition of the compounds was determined by varying the concentrations of *p*NPP (at least seven concentrations ranging from 0.2 and 20 mM) for each concentration of compound (at least three concentrations ranging from 0.1 and 0.3 μM or 3, 5 and 7 μM), and determining the initial rates of the corresponding reactions. The reaction rates were expressed as specific activity of the protein (μmol *p*NP·min$^{-1}$·mg$^{-1}$). The *p*-nitrophenol released was quantified and analyzed by fitting of the data to the Michaelis-Menten equation. The kinetic parameters $K_i$ were calculated by nonlinear fitting of the data to the competitive or non-competitive model inhibition equation. All data was plotted using GraphPad Prism software. The $K_i$ values have been achieved by the average of at least three independent experiments.[31]

### 4.5. Steady-State Fluorescence Measurements

Fluorescence measurements were carried out on a JASCO J-815 spectropolarimeter equipped with a Peltier temperature control, and a fluorescence detection unit in a 1 cm path length quartz cuvette at 25 °C. Emission spectra were recorded for wavelengths ranging from 300 to 450 nm, and the excitation of the samples was done at 280 or 295 nm. The intrinsic fluorescence emission spectra of PtpB, at a fixed concentration of 5 μM, were monitored in 20 mM Tris-HCl, pH 7.4, 50 mM NaCl, 2% (v/v) glycerol, and 1 mM 2-mercaptoethanol. The protein solution (300 μL) was titrated with an increasing concentration of the respective inhibitor, each time a 1 μL addition of the inhibitor was made. Two consecutive spectra were accumulated, and the contribution of the buffer plus inhibitor was subtracted. Two independent experiments were performed. The change in the intrinsic fluorescence signal of PtpB upon inhibitor binding was used to obtain the binding isotherm of the protein-inhibitor complex. The fluorescence data collected was analyzed with the following equation (eq 1), using the fluorescence intensity at spectral maxima (330 nm).

The resulting binding isotherms for the PtpB−inhibitor complex were analyzed via the complete solution of the equation (eq 1).[68]

$$\log \frac{(F_0-F)}{F} = \log K_a + n \log[I] \quad (1)$$

where $F_0$ and F are the fluorescence intensities before and after the addition of the inhibitor, [I] is the total inhibitor concentration. The inner-filter effect was corrected using the following factor (eq 2).[68]

$$F_{corr} = F_{obs} * 10^{\frac{A_{exc}+A_{em}}{2}} \quad (2)$$

where $F_{corr}$ is the corrected fluorescence value, $F_{obs}$ the measured fluorescence value, $A_{exc}$ the absorption value at the excitation wavelength, and $A_{em}$ the absorption value at the emission wavelength. The ultraviolet–visible (UV–vis) spectra were recorded on a UV–vis spectrophotometer (Ultrospec 2100 pro, Amersham Biosciences) at 25 °C in the range of 260–450 nm using a quartz cuvette with 1 cm path length.

**4.6. Isothermal Titration Calorimetry (ITC)**

Isothermal titration calorimetry (ITC) measurements of inhibitor binding to protein were recorded at 25 °C using a VP-ITC microcalorimeter (Microcal, GE Healthcare) in 20 mM Tris-HCl, pH 7.4, 50 mM NaCl, 2% (v/v) glycerol, 1 mM 2-mercaptoethanol and 5% (v/v) DMSO. PtpB sample was previously buffer exchanged into 20 mM Tris-HCl, pH 7.4, 50 mM NaCl, 2% (v/v) glycerol and 1 mM 2-mercaptoethanol using an ultrafiltration device (Amicon Ultra-15 Millipore 10 kDa). Protein concentration was determined by absorbance at 280 nm, using the calculated molar absorption coefficient of 14,440 $M^{-1}$ $cm^{-1}$. DMSO concentration in the protein solution was adjusted to 5% (v/v) before binding experiments were performed. Final ligand solution was obtained by dilution 1:50 (v/v) in the same buffer resulting in a final DMSO concentration of 5% (v/v). The titrations were performed using 10 μM PtpB solution in the sample cell and 200 μM compound solution in the syringe. A typical experiment consisted of 28 injections under the following parameters: one injection of 2 μL (for 4 s) followed by 27 injections of 10 μL (for 20 s); 150 s spacing between injections; 351 rpm stirring speed;

and reference power set to 15 μcal $s^{-1}$. The heat of dilution of the ligand into the buffer measured independently was essentially similar to the heat signal obtained at the end of the titration; so the signal of the last injection was used as the background heat signal. The experimental data were analyzed using the Origin 7.0 software, provided by MicroCal, and fitted using the one-site binding model. All the final values were the average obtained from two independent experiments. Values of ΔG° and $K_d$ were calculated using the thermodynamic relationships $\Delta G° = -RT \ln K_a$, and $K_d = 1/K_a$.

**4.7. Mass Spectrometry Analysis**

PtpB and PTP1B (5 μM) was preincubated with compounds (0, 100, or 400 μM) for 10 min at room temperature in 25 mM $NH_4HCO_3$ (pH 7.5) with 1% (v/v) DMSO before the addition of trypsin (10 μg/mL with a protease:protein ratio of 1:50). The protein-inhibitor complex was digested with trypsin at 37 °C for 2-3 hours. Proteolysis was stopped by homogenizing the reaction in the matrix solution of α-cyano-4-hydroxycinnamic acid (5 mg/mL in 50% (v/v) acetonitrile, and 0.1% (v/v) trifluoroacetic acid). Analyzes of the peptides were performed on a MALDI-TOF/TOF Autoflex III Smartbean™ spectrometer (Bruker Daltonics) in positive reflector mode using a pulsed 200 Hz laser with a wavelength of 355 nm. Source 1 voltage was set at 19 kV with a grid voltage of 16.6 kV. The standard peptides used for calibration ranged from 0.8 to 4 kDa (Peptide Calibration Standard, Bruker Daltonics). One single mass spectrum was formed from 8 subspectra per spot using 500 accepted laser impulses each. The generated spectra were analyzed using FlexAnalysis 3.3 software (Bruker Daltonics). The samples were identified comparing their peptide mass fingerprint profile and the mass list derived from the theoretical tryptic peptides. Two independent experiments were performed.

**4.8. Molecular modeling**

The possible binding mode and theoretical affinity of natural products against the catalytic site of PtpB were investigated by molecular modeling, using the procedure described previously.[31] Briefly, the crystallographic structure of PtpB in complex with a small molecule inhibitor (PDB ID: 2OZ5)[20] was

energy minimized in explicit solvent,[31] and used as rigid receptor in molecular docking simulations. The GOLD docking program (version 5.2.2) was used, while the GoldScore function was selected to score and rank ligand poses.[69]

**4.9. Macrophage assay**

The activity of Kuwanon G and Kuwanon H against Mtb in human macrophages was evaluated as previously described with minor modifications.[70, 71]. The human acute monocytic leukemia cell line THP-1 was obtained from the Biobanking of the Veterinary Resource (BVR, EZSLER, Brescia, Italy). Cells were grown in RPMI 1640 (Gibco, Thermo Fisher Scientific, Waltham, MA) with L-glutamine (Gibco) and 25 nM HEPES buffer supplemented with 10% heat-inactivated fetal calf serum (FCS, Gibco), penicillin 50 IU/mL (Sigma-Aldrich Co., St. Louis, MO) and streptomycin 50 µg/mL (Sigma-Aldrich) at 37 °C in 5% $CO_2$. Cells (2 x $10^5$) were therefore seeded in 24-well plates and incubated until reaching macrophage differentiation by treatment with 100 nM of phorbol-12-myristate-13-acetate (PMA, Sigma-Aldrich) for 10 h at 37 °C in 5% $CO_2$. The supernatant was discharged, fresh medium containing PMA was added again, and culture was incubated for an additional 4-day period. Mtb H37Ra ATCC 25177 was grown in Middlebrook 7H9 broth (Difco, Becton Dickinson, Sparks, MD) supplemented with 10% albumin, dextrose, and catalase (ADC, Difco), and 0.25% Tween 80 to minimize clump formation. Cells were harvested by centrifugation with 5 mm glass beads, resuspended in fresh medium and the titer adjusted to 3 x $10^6$ cells/mL by comparison with a McFarland No. 1 turbidity standard. Disaggregation of clumps was checked by Ziehl-Neelsen staining. The inoculum titer was also confirmed by plating 50 µL of the suspension onto Middlebrook 7H11 agar plates (Difco), supplemented with oleic acid, albumin, dextrose and catalase (OADC, Difco) after incubation at 37 °C in 5% $CO_2$ for 21 days. After differentiation, macrophages were washed with RPMI 1640 with no antibiotic, the number of cells per well was determined by an automated cell counter (Countess, Invitrogen, Thermo Fisher), and infected with 100 µL of Mtb for 3 h at 37 °C at a multiplicity of 1:1.

Macrophages were then washed three times with fresh medium and then incubated with 1 mL/well of supplemented RPMI 1640 with 10% FCS containing the testing compound with no antibiotics. Plates were incubated for 72 h at 37 °C in 5% $CO_2$ in order to allow bacteria to grow inside the macrophages. Cells were then washed and lysed by treatment with sodium dodecyl sulfate (SDS, Sigma-Aldrich) 0.05% in phosphate buffered saline solution at room temperature for 10 min. Lysates were therefore diluted in Middlebrook 7H9 medium, and 50 µL were seeded onto Middlebrook 7H11 supplemented with OADC. Plates were incubated at 37 °C in 5% $CO_2$ for 21 days, and the number of bacteria was determined by quantification of CFU.

**4.10. Cytotoxicity evaluation**

Toxicity of the tested compounds was determined against THP-1 cells seeded in 96-well plates at a density of 6 x $10^4$ cells/well in RPMI 1640 with HEPES 25 nM after differentiation with PMA 200 µM as described above. Cells were treated with Kuwanon G and Kuwanon H in RPMI 1640 at concentrations ranging between 0.78 and 200 µg/mL for 72 h in 5% $CO_2$ at 37 °C. Cells were then treated with 100 µL/well of a solution of MTT 1 mg/mL in PBS for 3 h at 37 °C and then the formazan product by MTT reduction was resuspended by treatment of 100 µL of a mixture obtained with NP40 5% and HCl 0.04 N in isopropanol. The 50% cell-inhibitory concentration ($CC_{50}$), considered as the reduction by 50% of the optical density values ($OD_{540,690}$) with respect to control non-treated cells, was obtained using an automatic plate reader.

**4.11. Determination of the minimum inhibitory concentration (MIC)**

MICs of Kuwanon G and Kuwanon H were determined against Mtb H37Ra ATCC 25197 by the resazurin microtiter assay as previously described[72, 73] with slight modifications. The assay was performed in 96-well microplates. To 100 µL of Middlebrook 7H9 medium supplemented with ADC containing Kuwanon G and Kuwanon H at concentrations ranging between 0.25 and 128 µg/mL were added the same volume of a suspension of Mtb prepared as described above to obtain final

concentrations of compounds ranging between 0.125 and 64 µg/mL and a final inoculum of 7 x $10^6$ cells/ml. Plates were incubated at 37 °C in $CO_2$ 5% for 7 days. 30 µL of resazurin solution prepared at 0.01% (w/v) in distilled water, filter sterilized and stored at 4 °C, was added to each well, incubated overnight at 37 °C, and assessed for color development. Isoniazid was used as a control.

### 4.12. Pan Assay Interference Compounds (PAINS) liability

The potential PAINS liability of compounds studied in this work was evaluated in agreement with the work of Baell and Holloway,[74] as well as by the online PAINS remover filter (http://cbligand.org/PAINS/). Notably, none of tested compounds of Figure 1 was classified as PAINS.

## 5. AUTHOR INFORMATION

### Corresponding Author

*Mattia Mori, Center for Life Nano Science@Sapienza, Istituto Italiano di Tecnologia, viale Regina Elena 291, 00161 Roma, Italy. Tel: +39 06 499 12778; email: m.mattia79@gmail.com

*Hernán Terenzi, Centro de Biologia Molecular Estrutural, CEBIME−UFSC, Universidade Federal de Santa Catarina, Campus Trindade, 88040-900, Florianopolis −SC, Brasil. Tel.: +55 48 3721 6426; Fax: +55 48 3721 9672; email: hernan.terenzi@ufsc.br

The authors report no conflicts of interest

## 6. ACKNOWLEDGMENTS

We thank the Center for Life Nano Science@Sapienza, Istituto Italiano di Tecnologia (IIT), Roma, Italy, and the Bilateral Projects 2016 between Sapienza Università di Roma (Italy) and Universidade Federal de Santa Catarina (Brazil) for financial support. The authors would like to acknowledge networking contribution by the COST Action CM1407 “Challenging organic syntheses inspired by nature - from natural products chemistry to drug discovery”. Special thanks are due to Prof. Dr. Pedro

M. Alzari (Institut Pasteur, Paris, France) for the PtpA and PtpB plasmids, Dr. Tiago A. S. Brandão (Universidade Federal de Minas Gerais, Brasil) for the PTP1B plasmid and Dr. Nunzio Bottini (University of Southern California, United States) for the PTP-PEST and LYP plasmids.

## 7. ASSOCIATED CONTENT

**Supporting Information.** Additional intrinsic fluorescence data and graphs, enzymatic inhibition graphs, UV-vis absorption spectra of PtpB in the presence and absence of compounds, expanded view of the mass spectra, graphs of the proteolytic protection of PtpB, and predicted binding mode data and figures.

## 8. REFERENCES

[1] WHO, World Health Organization. Global Tuberculosis Report 2016, in, Available in:<http://apps.who.int/iris/bitstream/10665/250441/1/9789241565394-eng.pdf?ua=1>. 2016.

[2] K. Rowland, Totally drug-resistant TB emerges in India, in: Nature News, http://www.nature.com/news/totally-drug-resistant-tb-emerges-in-india-1.9797, 2012.

[3] S.T. Cole, R. Brosch, J. Parkhill, T. Garnier, C. Churcher, D. Harris, S.V. Gordon, K. Eiglmeier, S. Gas, C.E. Barry Iii, F. Tekaia, K. Badcock, D. Basham, D. Brown, T. Chillingworth, R. Connor, R. Davies, K. Devlin, T. Feltwell, S. Gentles, N. Hamlin, S. Holroyd, T. Hornsby, K. Jagels, A. Krogh, J. McLean, S. Moule, L. Murphy, K. Oliver, J. Osborne, M.A. Quail, M.A. Rajandream, J. Rogers, S. Rutter, K. Seeger, J. Skelton, R. Squares, S. Squares, J.E. Sulston, K. Taylor, S. Whitehead, B.G. Barrell, Deciphering the biology of mycobacterium tuberculosis from the complete genome sequence, Nature, 393 (1998) 537-544.

[4] A. Sajid, G. Arora, A. Singhal, V.C. Kalia, Y. Singh, Protein Phosphatases of Pathogenic Bacteria: Role in Physiology and Virulence, Annu. Rev. Microbiol., 69 (2015) 527-547.

[5] A. Mascarello, L.D. Chiaradia-Delatorre, M. Mori, H. Terenzi, B. Botta, Mycobacterium tuberculosis-secreted tyrosine phosphatases as targets against tuberculosis: exploring natural sources in searching for new drugs, Curr. Pharm. Des., (2016).

[6] A. Caselli, P. Paoli, A. Santi, C. Mugnaioni, A. Toti, G. Camici, P. Cirri, Low molecular weight protein tyrosine phosphatase: Multifaceted functions of an evolutionarily conserved enzyme, Biochim. Biophys. Acta, 1864 (2016) 1339-1355.

[7] A. Koul, T. Herget, B. Klebl, A. Ullrich, Interplay between mycobacteria and host signalling pathways, Nat. Rev. Microbiol., 2 (2004) 189-202.

[8] J. Wang, B.X. Li, P.P. Ge, J. Li, Q. Wang, G.F. Gao, X.B. Qiu, C.H. Liu, Mycobacterium tuberculosis suppresses innate immunity by coopting the host ubiquitin system, Nat. Immunol., 16 (2015) 237-245.

[9] J. Wang, J.L.L. Teng, D.D. Zhao, P.P. Ge, B.X. Li, P.C.Y. Woo, C.H. Liu, The ubiquitin ligase TRIM27 functions as a host restriction factor antagonized by Mycobacterium tuberculosis PtpA during mycobacterial infection, Scientific Reports, 6 (2016).

[10] R. Guler, F. Brombacher, Host-directed drug therapy for tuberculosis, Nat. Chem. Biol., 11 (2015) 748-751.

[11] H. Bach, K.G. Papavinasasundaram, D. Wong, Z. Hmama, Y. Av-Gay, Mycobacterium tuberculosis Virulence Is Mediated by PtpA Dephosphorylation of Human Vacuolar Protein Sorting 33B, Cell Host Microbe, 3 (2008) 316-322.

[12] D. Wong, H. Bach, J. Sun, Z. Hmama, Y. Av-Gay, Mycobacterium tuberculosis protein tyrosine phosphatase (PtpA) excludes host vacuolar-H +-ATPase to inhibit phagosome acidification, Proc. Natl. Acad. Sci. U. S. A., 108 (2011) 19371-19376.

[13] N.J. Beresford, D. Mulhearn, B. Szczepankiewicz, G. Liu, M.E. Johnson, A. Fordham-Skelton, C. Abad-Zapatero, J.S. Cavet, L. Tabernero, Inhibition of MptpB phosphatase from Mycobacterium

tuberculosis impairs mycobacterial survival in macrophages, J. Antimicrob. Chemother., 63 (2009) 928-936.

[14] B. Zhou, Y. He, X. Zhang, J. Xu, Y. Luo, Y. Wang, S.G. Franzblau, Z. Yang, R.J. Chan, Y. Liu, J. Zheng, Z.-Y. Zhang, Targeting mycobacterium protein tyrosine phosphatase B for antituberculosis agents, Proceedings of the National Academy of Sciences, 107 (2010) 4573-4578.

[15] A. Mascarello, L.D. Chiaradia, J. Vernal, A. Villarino, R.V.C. Guido, P. Perizzolo, V. Poirier, D. Wong, P.G.A. Martins, R.J. Nunes, R.A. Yunes, A.D. Andricopulo, Y. Av-Gay, H. Terenzi, Inhibition of Mycobacterium tuberculosis tyrosine phosphatase PtpA by synthetic chalcones: Kinetics, molecular modeling, toxicity and effect on growth, Bioorg. Med. Chem., 18 (2010) 3783-3789.

[16] D. Wong, J.D. Chao, Y. Av-Gay, Mycobacterium tuberculosis-secreted phosphatases: from pathogenesis to targets for TB drug development, Trends Microbiol., 21 (2013) 100-109.

[17] N.K. Dutta, R.J. He, M.L. Pinn, Y.T. He, F. Burrows, Z.Y. Zhang, P.C. Karakousis, Mycobacterial Protein Tyrosine Phosphatases A and B Inhibitors Augment the Bactericidal Activity of the Standard Anti-tuberculosis Regimen, Acs Infectious Diseases, 2 (2016) 231-239.

[18] L. Chen, B. Zhou, S. Zhang, L. Wu, Y.H. Wang, S.G. Franzblau, Z.Y. Zhang, Identification and Characterization of Novel Inhibitors of mPTPB, an Essential Virulent Phosphatase from Mycobacterium tuberculosis, ACS Medicinal Chemistry Letters, 1 (2010) 355-359.

[19] K.A. Rawls, P. Therese Lang, J. Takeuchi, S. Imamura, T.D. Baguley, C. Grundner, T. Alber, J.A. Ellman, Fragment-based discovery of selective inhibitors of the Mycobacterium tuberculosis protein tyrosine phosphatase PtpA, Bioorg. Med. Chem. Lett., 19 (2009) 6851-6854.

[20] C. Grundner, D. Perrin, R. Hooft van Huijsduijnen, D. Swinnen, J. Gonzalez, C.L. Gee, T.N. Wells, T. Alber, Structural basis for selective inhibition of Mycobacterium tuberculosis protein tyrosine phosphatase PtpB, Structure, 15 (2007) 499-509.

[21] M.B. Soellner, K.A. Rawls, C. Grundner, T. Alber, J.A. Ellman, Fragment-Based Substrate Activity Screening Method for the Identification of Potent Inhibitors of the Mycobacterium tuberculosis Phosphatase PtpB, J. Am. Chem. Soc., 129 (2007) 9613-9615.

[22] V.V. Vintonyak, K. Warburg, B. Over, K. Hübel, D. Rauh, H. Waldmann, Identification and further development of thiazolidinones spiro-fused to indolin-2-ones as potent and selective inhibitors of Mycobacterium tuberculosis protein tyrosine phosphatase B, Tetrahedron, 67 (2011) 6713-6729.

[23] L.F. Zeng, J. Xu, Y. He, R. He, L. Wu, A.M. Gunawan, Z.Y. Zhang, A Facile Hydroxyindole Carboxylic Acid Based Focused Library Approach for Potent and Selective Inhibitors of Mycobacterium Protein Tyrosine PhosphataseB, ChemMedChem, 8 (2013) 904-908.

[24] E. Sieniawska, Targeting Mycobacterial Enzymes with Natural Products, Chem. Biol., 22 (2015) 1288-1300.

[25] A. Harvey, Strategies for discovering drugs from previously unexplored natural products, Drug Discov. Today, 5 (2000) 294-300.

[26] A.L. Harvey, R. Edrada-Ebel, R.J. Quinn, The re-emergence of natural products for drug discovery in the genomics era, Nat. Rev. Drug Discov., 14 (2015) 111-129.

[27] M. Mori, C.T. Supuran, Editorial: Challenging Organic Syntheses and Pharmacological Applications of Natural Products and their Derivatives, Curr. Pharm. Des., 21 (2015) 5451-5452.

[28] M. Mori, C.T. Supuran, Editorial: Challenging Organic Syntheses and Pharmacological Applications of Natural Products and their Derivatives - Part II, Curr. Pharm. Des., 22 (2016) 1559-1560.

[29] L.D. Chiaradia, A. Mascarello, M. Purificação, J. Vernal, M.N.S. Cordeiro, M.E. Zenteno, A. Villarino, R.J. Nunes, R.A. Yunes, H. Terenzi, Synthetic chalcones as efficient inhibitors of Mycobacterium tuberculosis protein tyrosine phosphatase PtpA, Bioorg. Med. Chem. Lett., 18 (2008) 6227-6230.

[30] L.D. Chiaradia, P.G.A. Martins, M.N.S. Cordeiro, R.V.C. Guido, G. Ecco, A.D. Andricopulo, R.A. Yunes, J. Vernal, R.J. Nunes, H. Terenzi, Synthesis, biological evaluation, and molecular modeling of chalcone derivatives as potent inhibitors of Mycobacterium tuberculosis protein tyrosine phosphatases (PtpA and PtpB), J. Med. Chem., 55 (2012) 390-402.

[31] A. Mascarello, M. Mori, L.D. Chiaradia-Delatorre, A.C.O. Menegatti, F.D. Monache, F. Ferrari, R.A. Yunes, R.J. Nunes, H. Terenzi, B. Botta, M. Botta, Discovery of *Mycobacterium tuberculosis* Protein Tyrosine Phosphatase B (PtpB) Inhibitors from Natural Products, PLoS ONE, 8 (2013) e77081.

[32] F. Ferrari, B. Monacelli, I. Messana, Comparison between in vivo and in vitro metabolite production of Morus nigra, Planta Med., 65 (1999) 85-87.

[33] V. Iovine, I. Benni, R. Sabia, I. D'Acquarica, G. Fabrizi, B. Botta, A. Calcaterra, Total Synthesis of (+/-)-Kuwanol E, J. Nat. Prod., 79 (2016) 2495-2503.

[34] T. Fukai, K. Kaitou, S. Terada, Antimicrobial activity of 2-arylbenzofurans from Morus species against methicillin-resistant Staphylococcus aureus, Fitoterapia, 76 (2005) 708-711.

[35] T. Nomura, Y. Hano, T. Fukai, Chemistry and biosynthesis of isoprenylated flavonoids from Japanese mulberry tree, Proceedings of the Japan Academy Series B: Physical and Biological Sciences, 85 (2009) 391-408.

[36] Y. Yang, Y.X. Tan, R.Y. Chen, J. Kang, The latest review on the polyphenols and their bioactivities of Chinese Morus plants, J. Asian Nat. Prod. Res., 16 (2014) 690-702.

[37] H.P. Huang, T.T. Ou, C.J. Wang, Mulberry (Sang Shèn Zǐ) and its bioactive compounds, the chemoprevention effects and molecular mechanisms in vitro and in vivo, Journal of Traditional and Complementary Medicine, 3 (2013) 7-15.

[38] Z.P. Zheng, K.W. Cheng, Q. Zhu, X.C. Wang, Z.X. Lin, M. Wang, Tyrosinase inhibitory constituents from the roots of Morus nigra: A structure-activity relationship study, J. Agric. Food Chem., 58 (2010) 5368-5373.

[39] Z. Yang, Y. Zhang, L. Sun, Y. Wang, X. Gao, Y. Cheng, An ultrafiltration high-performance liquid chromatography coupled with diode array detector and mass spectrometry approach for screening and characterising tyrosinase inhibitors from mulberry leaves, Anal. Chim. Acta, 719 (2012) 87-95.

[40] X. Zhang, X. Hu, A. Hou, H. Wang, Inhibitory effect of 2,4,2′,4′-tetrahydroxy-3-(3-methyl-2-butenyl)-chalcone on tyrosinase activity and melanin biosynthesis, Biol. Pharm. Bull., 32 (2009) 86-90.

[41] S.K. Chen, P. Zhao, Y.X. Shao, Z. Li, C. Zhang, P. Liu, X. He, H.B. Luo, X. Hu, Moracin M from Morus alba L. is a natural phosphodiesterase-4 inhibitor, Bioorg. Med. Chem. Lett., 22 (2012) 3261-3264.

[42] Z. Yu, P.F. Wing, C.H.K. Cheng, The dual actions of morin (3,5,7,2′,4′-pentahydroxyflavone) as a hypouricemic agent: Uricosuric effect and xanthine oxidase inhibitory activity, J. Pharmacol. Exp. Ther., 316 (2006) 169-175.

[43] Y.L. Zhang, J.G. Luo, C.X. Wan, Z.B. Zhou, L.Y. Kong, Geranylated 2-arylbenzofurans from Morus alba var. tatarica and their α-glucosidase and protein tyrosine phosphatase 1B inhibitory activities, Fitoterapia, 92 (2014) 116-126.

[44] G.N. Kim, Y.I. Kwon, H.D. Jang, Mulberry leaf extract reduces postprandial hyperglycemia with few side effects by inhibiting α-glucosidase in normal rats, J. Med. Food, 14 (2011) 712-717.

[45] D.M. Hoang, T.M. Ngoc, N.T. Dat, D.T. Ha, Y.H. Kim, H.V. Luong, J.S. Ahn, K. Bae, Protein tyrosine phosphatase 1B inhibitors isolated from Morus bombycis, Bioorg. Med. Chem. Lett., 19 (2009) 6759-6761.

[46] L. Wang, H.Q. Wang, R.Y. Chen, Studies on chemical constituents from bark of Morus nigra, Zhongguo Zhongyao Zazhi, 32 (2007) 2497-2499.

[47] R.A. Copeland, Evaluation of enzyme inhibitors in drug discovery. A guide for medicinal chemists and pharmacologists, Methods of biochemical analysis., 46 (2005) 1-265.

[48] C. Grundner, H.L. Ng, T. Alber, Mycobacterium tuberculosis protein tyrosine phosphatase PtpB structure reveals a diverged fold and a buried active site, Structure, 13 (2005) 1625-1634.

[49] J.R. Lakowicz, Principles of Fluorescence Spectroscopy, 3 ed., Springer US, 2006.

[50] D.R. Banerjee, D. Dutta, B. Saha, S. Bhattacharyya, K. Senapati, A.K. Das, A. Basak, Design, synthesis and characterization of novel inhibitors against mycobacterial [small beta]-ketoacyl CoA reductase FabG4, Org. Biomol. Chem., 12 (2014) 73-85.

[51] R.K. Singh, N. Lall, T.S. Leedahl, A. McGillivray, T. Mandal, M. Haldar, S. Mallik, G. Cook, D.K. Srivastava, Kinetic and thermodynamic rationale for suberoylanilide hydroxamic acid being a preferential human histone deacetylase 8 inhibitor as compared to the structurally similar ligand, trichostatin A, Biochemistry, 52 (2013) 8139-8149.

[52] Y. Kawasaki, E. Freire, Finding a better path to drug selectivity, Drug Discov. Today, 16 (2011) 985-990.

[53] X. Hu, M. Vujanac, C.E. Stebbins, Computational analysis of tyrosine phosphatase inhibitor selectivity for the virulence factors YopH and SptP, J. Mol. Graph. Model., 23 (2004) 175-187.

[54] C. Wiesmann, K.J. Barr, J. Kung, J. Zhu, D.A. Erlanson, W. Shen, B.J. Fahr, M. Zhong, L. Taylor, M. Randal, R.S. McDowell, S.K. Hansen, Allosteric inhibition of protein tyrosine phosphatase 1B, Nat. Struct. Mol. Biol., 11 (2004) 730-737.

[55] N. Krishnan, D. Koveal, D.H. Miller, B. Xue, S.D. Akshinthala, J. Kragelj, M.R. Jensen, C.M. Gauss, R. Page, M. Blackledge, S.K. Muthuswamy, W. Peti, N.K. Tonks, Targeting the disordered C terminus of PTP1B with an allosteric inhibitor, Nat. Chem. Biol., 10 (2014) 558-566.

[56] M.A. Ghattas, N. Raslan, A. Sadeq, M. Al Sorkhy, N. Atatreh, Druggability analysis and classification of protein tyrosine phosphatase active sites, Drug Des. Devel. Ther., 10 (2016) 3197-3209.

[57] D.S. Cui, V. Beaumont, P.S. Ginther, J.M. Lipchock, J.P. Loria, Leveraging Reciprocity to Identify and Characterize Unknown Allosteric Sites in Protein Tyrosine Phosphatases, J. Mol. Biol., 429 (2017) 2360-2372.

[58] T. Nomura, T. Fukai, Y. Hano, S. Terada, T. Kuramochi, Constituents of Cultivated Mulberry Tree. XII. Isolation of Two New Natural Diels-Alder Adducts from Root Bark of Morus alba., Planta Med., 47 (1983) 151−156.

[59] Y. Hano, S. Suzuki, H. Kohno, T. Nomura, Absolute-Configuration of Kuwanon-L, a Natural Diels-Alder Type Adduct from the Morus Root Bark, Heterocycles, 27 (1988) 75-81.

[60] T. Nomura, Phenolic compounds of the mulberry tree and related plants, Fortschr. Chem. Org. Naturst., 53 (1988) 87-201.

[61] L. Shi-De, J. Nemec, N. Bing-Mei, Anti-HIV flavonoids from Morus alba. , Acta Bot. Yunnanica, 17 (1995) 89−95.

[62] T. Fujimoto, T. Nomura, Structures of cudraflavanone A and euchrestaflavanone C. , Heterocycles, 22 (1984) 997-1003.

[63] W.F. Yi, J.B. Peng, G. Ren, W. Jiang, J. Liang, W.J. Yuan, [Chemical Constitutes from Root of Artocarpus styracifolius], Zhong Yao Cai, 38 (2015) 972-974.

[64] T. Fukai, Y. Hano, K. Hirakura, T. Nomura, J. Uzawa, K. Fukushima, Structures of two natural hypotensive Diels-Alder type adducts, mulberrofurans F and G, from the cultivated mulberry tree (Morus lhou KOIDZ.), Chem. Pharm. Bull. (Tokyo), 33 (1985) 3195-3204.

[65] S. Ueda, T. Nomura, T. Fukai, J. Matsumoto, Kuwanon J, a new Diels-Alder adduct and chalcomoracin from callus culture of Morus alba L., Chem. Pharm. Bull., 30 (1982) 3042−3045.

[66] B.N. Su, M. Cuendet, M.E. Hawthorne, L.B. Kardono, S. Riswan, H.H. Fong, R.G. Mehta, J.M. Pezzuto, A.D. Kinghorn, Constituents of the bark and twigs of Artocarpus dadah with cyclooxygenase inhibitory activity, J. Nat. Prod., 65 (2002) 163-169.

[67] N.H. Soekamto, N. La Nafie, F.W. Mandey, M. Garson, Norartocarpetin, flavone derivative from leaves of Artocarpus fretessi, Indo. J. Med. , 9 (2009) 328−331.

[68] M. Van De Weert, Fluorescence quenching to study protein-ligand binding: Common errors, J. Fluoresc., 20 (2010) 625-629.

[69] M.L. Verdonk, J.C. Cole, M.J. Hartshorn, C.W. Murray, R.D. Taylor, Improved protein-ligand docking using GOLD, Proteins, 52 (2003) 609-623.

[70] E. Rey-Jurado, G. Tudo, D. Soy, J. Gonzalez-Martin, Activity and interactions of levofloxacin, linezolid, ethambutol and amikacin in three-drug combinations against Mycobacterium tuberculosis isolates in a human macrophage model, Int. J. Antimicrob. Agents, 42 (2013) 524-530.

[71] S.A. Theus, M.D. Cave, K.D. Eisenach, Activated THP-1 cells: An attractive model for the assessment of intracellular growth rates of Mycobacterium tuberculosis isolates, Infect. Immun., 72 (2004) 1169-1173.

[72] J.C. Palomino, A. Martin, M. Camacho, H. Guerra, J. Swings, F. Portaels, Resazurin microtiter assay plate: Simple and inexpensive method for detection of drug resistance in Mycobacterium tuberculosis, Antimicrob. Agents Chemother., 46 (2002) 2720-2722.

[73] N.K. Taneja, J.S. Tyagi, Resazurin reduction assays for screening of anti-tubercular compounds against dormant and actively growing Mycobacterium tuberculosis, Mycobacterium bovis BCG and Mycobacterium smegmatis, J. Antimicrob. Chemother., 60 (2007) 288-293.

[74] J.B. Baell, G.A. Holloway, New Substructure Filters for Removal of Pan Assay Interference Compounds (PAINS) from Screening Libraries and for Their Exclusion in Bioassays, J. Med. Chem., 53 (2010) 2719-2740.

## Highlights

- Novel PtpB inhibitors extracted from *Morus nigra* are described;
- PtpB binding is characterized by multiple biochemical and spectroscopic tools;
- Anti-tubercular activity was evaluated on lead candidates;
- Two compounds emerged as sub-micromolar PtpB inhibitors, one active in macrophages.